Am J Physiol Cell Physiol 285: C119–C128, 2003.
First published March 12, 2003; 10.1152/ajpcell.00296.2002.

SH oxidation coordinates subunits of rat brain ryanodine receptor channels activated by calcium and ATP

Ricardo Bull,[1] Juan José Marengo,[1,2] José Pablo Finkelstein,[1] María Isabel Behrens,[1,3] and Osvaldo Alvarez[4]

[1]*Programa de Fisiología y Biofísica and* [2]*Programa de Patología, Instituto de Ciencias Biomédicas, Facultad de Medicina, Universidad de Chile, Santiago 838-0453;* [3]*Servicio de Neurología, Hospital Sótero del Río, Santiago 820-7257; and* [4]*Departamento de Biología, Facultad de Ciencias, Universidad de Chile, Santiago, Chile 780-0024*

Submitted 25 June 2002; accepted in final form 4 March 2003

Bull, Ricardo, Juan José Marengo, José Pablo Finkelstein, María Isabel Behrens, and Osvaldo Alvarez. SH oxidation coordinates subunits of rat brain ryanodine receptor channels activated by calcium and ATP. *Am J Physiol Cell Physiol* 285: C119–C128, 2003. First published March 12, 2003; 10.1152/ajpcell.00296.2002.—We have reported that ryanodine receptor (RyR) channels display three different responses to cytoplasmic free Ca^{2+} concentration ($[Ca^{2+}]$) depending on their redox state (Marengo JJ, Hidalgo C, and Bull R. *Biophys J* 74: 1263–1277, 1998), with low, moderate, and high maximal fractional open times (P_o). Activation by ATP of single RyR channels from rat brain cortex was tested in planar lipid bilayers with 10 or 0.1 μM cytoplasmic $[Ca^{2+}]$. At 10 μM $[Ca^{2+}]$, low-P_o channels presented lower apparent affinity to activation by ATP [[ATP] for half-maximal activation (K_{aATP}) = 422 μM] than moderate-P_o channels (K_{aATP} = 82 μM). Oxidation of low-P_o channels with thimerosal or 2,2′-dithiodipyridine (DTDP) gave rise to moderate-P_o channels and decreased K_{aATP} from 422 to 82 μM. At 0.1 μM cytoplasmic $[Ca^{2+}]$, ATP induced an almost negligible activation of low-P_o channels. After oxidation to high-P_o behavior, activation by ATP was markedly increased. Noise analysis of single-channel fluctuations of low-P_o channels at 10 μM $[Ca^{2+}]$ plus ATP revealed the presence of subconductance states, suggesting a conduction mechanism that involves four independent subchannels. On oxidation the subchannels opened and closed in a concerted mode.

subconductance states; calcium ion release channels; calcium ion regulation; thimerosal; 2,2′-dithiodipyridine

RYANODINE RECEPTOR (RyR) channels form a pathway that allows the release of calcium from endoplasmic reticulum (ER) and/or sarcoplasmic reticulum (SR) to the cytoplasm. This process underlies many cellular responses, such as contraction in skeletal and cardiac muscle (14, 41, 57) and synaptic plasticity and gene expression in neurons (5, 6, 10, 24). RyR channels are activated by several cytoplasmic agonists and/or modulators such as Ca^{2+} and ATP and by caffeine (4, 41, 57).

RyR channels are coded by three different genes in mammalian tissue. *RyR-1* is the most abundant isoform expressed in skeletal muscle (23, 40, 41, 57); *RyR-2* is the most abundant isoform expressed in heart and brain; and *RyR-3* is expressed in small amounts in brain and in a few adult skeletal muscle types (25, 42). Rat brain expresses the three known mammalian RyR genes (14, 23). All isoforms of RyR channels comprise four identical subunits. In addition, skeletal muscle RyR-1 has four molecules of FK-506 binding protein (FKBP)12 tightly associated, which stabilize the RyR-1 complex and allow the four subunits to open and close coordinately (8, 26, 44, 53). Moreover, FKBP mediates the coordination of two or more individual skeletal or cardiac muscle tetramers (37, 38).

RyR channels display multiple conductance states. This is especially evident in RyR-1 channels purified from skeletal muscle, which display subconductance levels of one-fourth, one-half, or three-fourths of the maximal channel conductance (33, 49). Recombinant RyR-1, when expressed in insect cells without the regulatory peptide FKBP12, forms channels displaying the same three subconductance states (8). The addition of FKBP12 stabilizes the channel complex, resulting in the formation of channels with full conductance (8, 44). Removal of FKBP by rapamycin or FK-506 reverses this stabilizing effect in RyR channels from skeletal and cardiac muscle (8, 28, 37, 38). FKBP12 is not tightly associated to RyR channels from brain (11).

Several studies performed in single channels obtained from cardiac or skeletal muscle and from brain tissue showed that RyR channels can display three types of responses to cytoplasmic calcium, low-, moderate-, and high-fractional open time (P_o) calcium dependence (12, 13, 22, 34, 48). Low-P_o behavior has a bell-shaped response with poor activation by calcium, reaching very low P_o (low-P_o channels) (34). Moderate-P_o behavior is also characterized by a bell-shaped calcium curve with marked activation at micromolar Ca^{2+} concentrations ($[Ca^{2+}]$) (48) and inhibition at

Address for reprint requests and other correspondence: R. Bull, Programa de Fisiología y Biofísica, ICBM, Facultad de Medicina, Universidad de Chile, Independencia 1027, ZIP 6530499, Casilla 70005, Correo 7, Santiago, Chile (E-mail: rbull@machi.med.uchile.cl).

The costs of publication of this article were defrayed in part by the payment of page charges. The article must therefore be hereby marked "*advertisement*" in accordance with 18 U.S.C. Section 1734 solely to indicate this fact.

$[Ca^{2+}] \geq 0.1$ mM (12, 22, 34). High-P_o behavior shows sigmoidal activation and absence of inhibition up to 0.5 mM $[Ca^{2+}]$ (12, 34). We previously reported (35) that RyR channels from skeletal muscle show the three types of calcium dependence, moderate- and low-P_o behavior being the most frequently encountered (13, 14, 35, 41). In cardiac tissue, only two calcium dependencies have been described, corresponding to moderate and high P_o; low-P_o behavior was never observed (35, 46). Isolated SR vesicles from brain tissue also show the three types of calcium dependence, the low-P_o response being the most frequent behavior, followed by the moderate-P_o response. The least frequently observed RyR channel behavior in brain is the high-P_o response (34).

We showed (35) that changes in the oxidation state of RyR channels induce changes in their calcium dependencies. Several reagents that oxidize, alkylate, or *S*-nitrosylate critical SH residues of the channel protein activate RyR channels in bilayers and increase vesicular Ca^{2+} release (1, 2, 15, 16, 18, 20, 21, 32, 50, 52). In particular, we showed (35) that the three calcium responses can be observed in the same single channel incorporated in the bilayer by modification of the redox state, implying that the different calcium dependencies can be displayed by a single isoform. SH oxidation also modifies channel modulation by other agonists and inhibitors (15, 43, 51, 54). Recent evidence suggests that RyR channels may function as intracellular redox sensors (19, 21, 54).

RyR-mediated calcium-induced calcium release (CICR) is becoming increasingly important for brain function, including synaptic plasticity and neurodegeneration (5, 7). However, brain RyR channels have been much less studied than their skeletal or cardiac counterparts. In this work we studied, at the single-channel level, the activation induced by ATP and calcium of native and oxidized RyR channels from rat brain endoplasmic reticulum. We found that ATP differentially activated RyR channels depending on their calcium response. At 10 μM $[Ca^{2+}]$, RyR channels revealed multiple subconductance states and SH oxidation induced a decrease in the frequency of these substates. Noise analysis of single-channel fluctuations suggests a conduction mechanism that involves four independent subchannels. After SH oxidation, the channel subunits gated in a concerted fashion, favoring closed and full open states. Part of this work was published previously in abstract form (36).

MATERIALS AND METHODS

All animal procedures used in this study complied with the "Guiding Principles for Research Involving Animals and Human Beings" of the American Physiological Society.

Isolation of membrane fractions. ER vesicles enriched in RyR were obtained from rat (Sprague-Dawley) brain cortex as described previously with dithiothreitol as the SH reducing agent during all steps of the preparation (34).

Channel recording and analysis. Planar phospholipid bilayers were painted with a mixture of palmitoyl-oleoyl-phosphatidylethanolamine (POPE), phosphatidylserine (PS), and phosphatidylcholine (PC) in the proportion POPE-PS-PC = 5:3:2. Lipids obtained from Avanti Polar Lipids (Birmingham, AL) were dissolved in decane to a final concentration of 33 mg/ml. ER vesicles were fused with the bilayer as described previously (9, 34). After fusion, the *cis* (cytoplasmic) compartment, where the vesicles were added, was perfused with 5–10 times the compartment volume of a solution containing 225 mM HEPES-Tris, pH 7.4. To obtain the desired cytoplasmic free $[Ca^{2+}]$, EGTA and/or *N*-(2-hydroxyethyl)-ethylenediamine-triacetic acid (HEDTA) were used. Free $[Ca^{2+}]$ values from stock solution were checked with a calcium electrode. For the experiments at 10 μM free $[Ca^{2+}]$, 10 mM total HEDTA was used. For the experiments at 0.1 μM $[Ca^{2+}]$, 0.5 mM total Ca^{2+} and 1.45 mM total HEDTA were used. The amounts of EGTA, ATP, and Ca^{2+} required for the desired free [ATP] and free $[Ca^{2+}]$ were calculated with the program WinMAXC (**www.stanford.edu/~cpatton/wmaxc.zip**). The *trans* (intrareticular) compartment was replaced with 40 mM Ca-HEPES, 10 mM Tris-HEPES, pH 7.4. The charge carrier was calcium. The experiments were carried out at room temperature (22–24°C), with membranes held at 0 mV. Voltage was applied to the *cis* compartment, and the *trans* compartment was held at virtual ground through an operational amplifier in a current-to-voltage configuration. Current signals were both recorded on tape and acquired online.

For analysis, data were filtered at 400 Hz (−3 dB) with an eight-pole low-pass Bessel-type filter (902 LPF; Frequency Devices, Haverhill, MA) and digitized at 2 kHz with a 12-bit analog-to-digital converter (Labmaster DMA interface; Scientific Solutions, Solon, OH) with Axotape software (Axon Instruments, Burlingame, CA). Fractional open times were computed from records of 60 s or longer with pCLAMP software (Axon Instruments). Fractional open time was calculated as P_o^* according to the following equation

$$P_o^* = I_{mean}/I_{max} \quad (1)$$

where I_{mean} is mean current and I_{max} corresponds to the current of the full open channel. I_{max} was measured as the mean current of at least eight full open events lasting >30 ms.

Channels were classified according to their calcium dependence as described previously (34). Activity was measured at least at 10 and 500 μM $[Ca^{2+}]$, because maximal activation is usually achieved near the first concentration and inhibition (if present) is clearly apparent at the second concentration. Low-P_o channels in the present study displayed P_o values <0.04 (0.017 ± 0.002; mean ± SE) at 10 μM $[Ca^{2+}]$. Moderate-P_o channels displayed P_o values >0.1 at 10 μM $[Ca^{2+}]$ (0.24 ± 0.03; mean ± SE) and were inhibited by 500 μM $[Ca^{2+}]$. High-P_o channels showed P_o values >0.75 at 10 μM $[Ca^{2+}]$ and were not inhibited by 500 μM $[Ca^{2+}]$.

For noise analysis, mean current and current variance were measured in successive periods lasting 1 s. Data pairs were fitted with a parabolic equation as described in RESULTS. It was verified that the noise analysis performed in a simulated channel generated with the model and kinetic constants reported by Zahradníková and Palade (55) for cardiac RyR channels was not affected by a cutoff filter of 400 Hz.

Thimerosal (10–20 μM) or 2,2′-dithiodipyridine (DTDP; 100 μM) was added to the cytoplasmic compartment until a change in P_o was observed (30–200 s), and the reaction was stopped by removal of the nonreacted reagent through extensive perfusion of the compartment (5–10 times the compartment volume) with a solution containing 225 mM HEPES-Tris, pH 7.4 (35).

Materials. Lipids were obtained from Avanti Polar Lipids. Protease inhibitors, ATP disodium salt, and other reagents were obtained from Sigma (St. Louis, MO).

RESULTS

Activation by ATP of native RyR channels. Single-channel current recordings of calcium-release channels were obtained after fusion of vesicles isolated from rat brain cortex with planar lipid bilayers. The full open state displayed a conductance of ~100 pS with 40 mM calcium in the luminal (*trans*) compartment, as previously reported (34). Channels were divided into low, moderate, or high P_o, according to their calcium dependence as described previously (Refs. 34 and 35; see MATERIALS AND METHODS). Activation by ATP of ryanodine-sensitive channels was studied. Most of the experiments were performed with low- and moderate-P_o channels at 10 μM cytoplasmic [Ca^{2+}]. Channels with high-P_o behavior were very infrequently observed. However, in the few experiments in which high-P_o channels were incorporated in the bilayer, activation by ATP was observed, but the low number of experiments (3), and the fact that at 10 μM [Ca^{2+}] they already have a high P_o, precluded calculation of the parameters of ATP activation. Therefore, the analysis was restricted to the low- and moderate-P_o channels. In the presence of ATP, both low- and moderate-P_o channels gated with fast kinetics between the closed state and poorly resolvable open states because of the low signal-to-noise ratio and the fast kinetics (Fig. 1, *fourth traces*). Current levels were better resolved in the moderate-P_o than in the low-P_o channels. Opening of the low-P_o channel to the full open state was occasionally observed at high [ATP] (see Fig. 1, *third trace*, *left*). To compare the activity of low-P_o and moderate-P_o channels, the fractional open time was calculated as P_o^* according to *Eq. 1* as described in MATERIALS AND METHODS. The addition of ryanodine induced the characteristic substate (~40% I_{max}, P_o ~1; Ref. 45), indicating that the channels studied indeed corresponded to single ryanodine-sensitive channels (data not shown).

ATP added to the cytoplasmic compartment activated spontaneous low-P_o and moderate-P_o channels at different concentrations, as illustrated in Fig. 1. Low-P_o channels required higher [ATP] to attain an extent of activation similar to that of moderate-P_o channels. Typical examples of activation by ATP of single RyR channels with low-P_o (*left*) or moderate-P_o

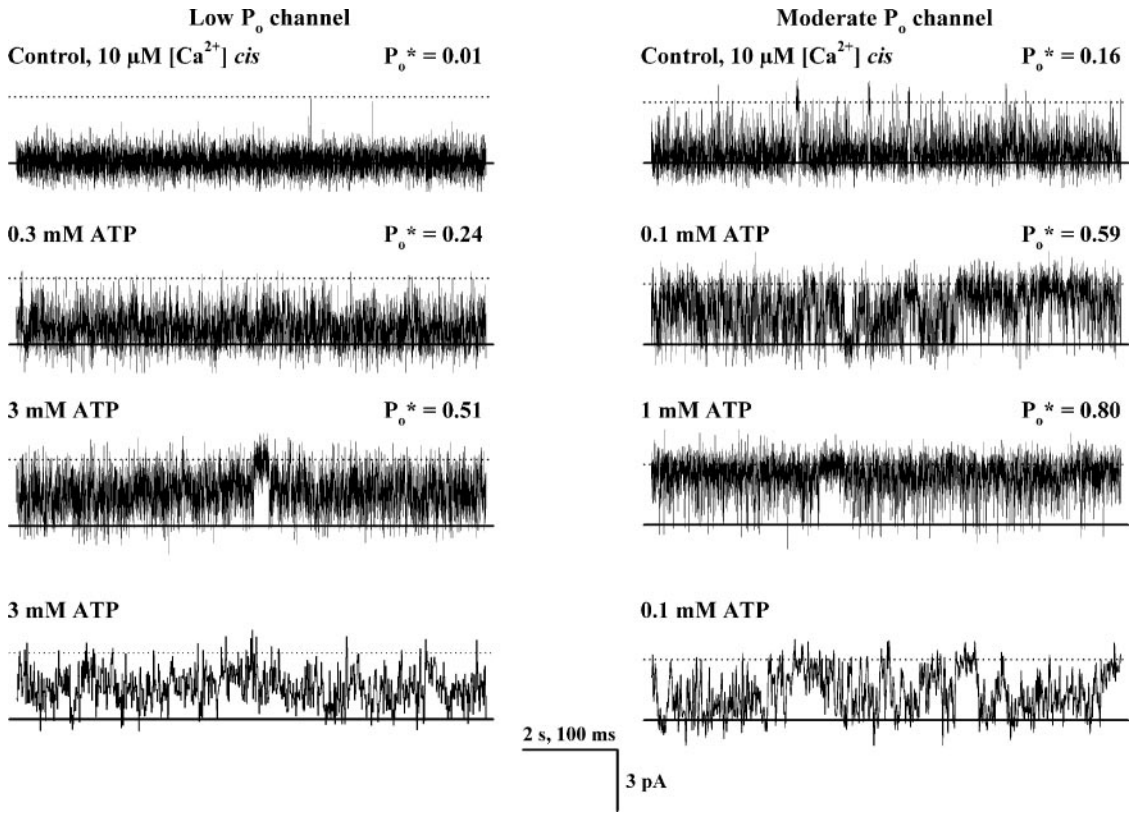

Fig. 1. Activation by ATP of native single ryanodine receptor (RyR) channels that displayed different responses to cytoplasmic Ca^{2+} concentration ([Ca^{2+}]). Representative current records were obtained at 10 μM cytoplasmic free [Ca^{2+}] with 10 mM *N*-(2-hydroxyethyl)ethylenediamine-triacetic acid (HEDTA) as calcium buffer. ATP was added to the cytoplasmic compartment of a single channel that displayed low-fractional open time (P_o^*) (*left*) or moderate-P_o (*right*) calcium dependence. Free [ATP] values and average P_o^* values, calculated from at least 180 s of continuous records, are given at the *top left* and *right*, respectively, of each trace. The *fourth traces* represent a selected segment of the *third* (*left*) or the *second* (*right*) *traces* in an expanded time scale. Horizontal calibration bars represent 2 s for *first 3 traces* and 100 ms for the *fourth traces* in both panels. Membrane was held at 0 mV. Channels open upward.

(*right*) calcium dependence are illustrated in Fig. 1. Representative current traces obtained in the presence of 10 μM cytoplasmic free [Ca^{2+}] are depicted for both channels, before (Fig. 1, *first traces*) and after addition of ATP at concentrations that induced about half-maximal activation (Fig. 1, *second traces*) and near maximal activation (Fig. 1, *third traces*), respectively. Addition of 0.3 mM ATP to the cytoplasmic compartment of the low-P_o channel increased P_o^* from 0.01 to 0.24, and 3 mM ATP further increased P_o^* to 0.51. Addition of 0.1 mM ATP to the moderate-P_o channel increased P_o^* from 0.16 to 0.59 and 1 mM ATP increased P_o^* to 0.80. P_o^* remained stable throughout the recording period at each [ATP] (see below). Occasionally (~10%), some channels changed their activity during the recording and were not included in the analysis.

Figure 2 shows activation curves for ATP of both types of channels depicting mean ± SD P_o^* values obtained with low-P_o ($N = 15$) or moderate-P_o ($N = 6$) channels. Two types of ATP dependence were observed: one for channels displaying low-P_o calcium dependence and the other for channels displaying moderate-P_o calcium dependence. Mean values were fitted with the following hyperbolic equation

$$P_o^* = P_{o\,in}^* + P_{o\,ATP}^* \cdot [ATP]/(K_{aATP} + [ATP]) \quad (2)$$

where $P_{o\,in}^*$ and $P_{o\,ATP}^*$ represent the fractional open time before addition of ATP and the maximal change in P_o^* induced by ATP, respectively, and K_{aATP} is the [ATP] for half-maximal activation of the channel. K_{aATP} of moderate-P_o channels was significantly lower than K_{aATP} of low-P_o channels (82 ± 15 vs. 422 ± 62 μM), whereas $P_{o\,ATP}^*$ values were similar (see Table 1). The data of individual experiments, in which P_o^* was measured at least at five different [ATP], were also fitted to *Eq. 2*. K_{aATP} values obtained ranged from 270 to 1,070 μM (580 ± 72 μM, mean ± SE; $N = 12$) for low-P_o channels and from 50 to 100 μM (76 ± 7 μM; $N = 4$) for moderate-P_o channels. Thus ATP activated both spontaneous low-P_o and moderate-P_o channels to a comparable extent but with about fivefold different K_{aATP} values.

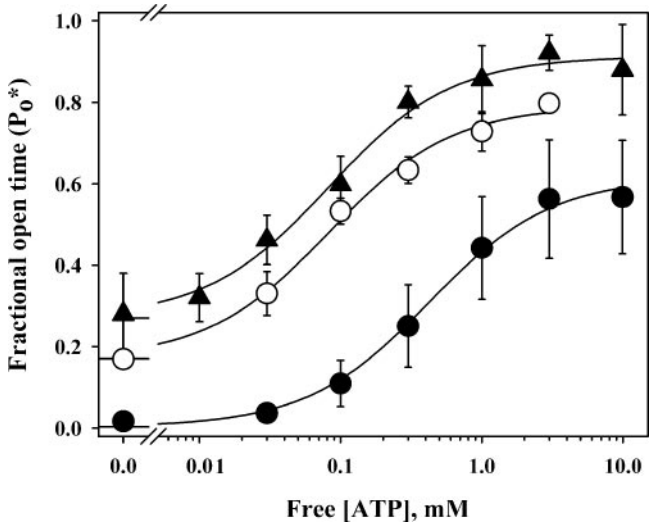

Fig. 2. Effect of cytoplasmic [ATP] on native and oxidized RyR channels. Native channels (circles): fractional open time (P_o^*) of channels spontaneously revealing low-P_o (filled circles) or moderate-P_o (open circles) calcium dependence is given as a function of cytoplasmic free [ATP]. Oxidized channels: filled triangles represent low-P_o channels that displayed moderate-P_o behavior after oxidation with thimerosal or 2,2′-dithiodipyridine (DTDP). The oxidizing agent was removed before recording as specified in MATERIALS AND METHODS. Symbols and error bars depict mean ± SD values. Solid lines represent the best nonlinear fits to *Eq. 2* (see text). Fitted parameters are displayed in Table 1.

Table 1. *Curve-fitting parameters for data of Fig. 2*

	K_{aATP}, μM	$P_{o\,in}^*$	$P_{o\,ATP}^*$
Low-P_o channels, native	422 ± 62	0.003 ± 0.001	0.612 ± 0.021
Moderate-P_o channels			
Native	82 ± 15	0.170 ± 0.024	0.621 ± 0.029
Oxidized	82 ± 14	0.271 ± 0.022	0.642 ± 0.026

Values were obtained from the nonlinear fit ± SE of the estimate. P_o, fractional open time; P_o^*, calculated P_o; $P_{o\,in}^*$, P_o^* before addition of ATP; $P_{o\,ATP}^*$, maximal ATP-induced change in P_o^*; K_{aATP}, ATP concentration for half-maximal activation.

Activation by ATP of oxidized RyR channels. Channels spontaneously presenting low-P_o behavior were oxidized to obtain moderate-P_o calcium dependence. Calcium dependence could be readily changed from low P_o to moderate P_o by treatment with the SH reagents thimerosal and DTDP, as reported previously (35). Figure 2 shows the activation curve induced by ATP, at 10 μM [Ca^{2+}], of single channels that attained moderate-P_o calcium dependence after incubation with thimerosal ($N = 4$) or DTDP ($N = 4$). There was no significant difference of ATP activation with these two reagents (K_{aATP} of 93 ± 12 and 78 ± 31 μM for DTDP and thimerosal, respectively), so they were pooled as a single group. The symbols in Fig. 2 represent mean ± SD values, and the continuous line through the symbols represents the nonlinear regression curve obtained with *Eq. 2*. There was no difference in K_{aATP} (82 ± 15 vs. 82 ± 14 μM) or in the extent of activation by ATP ($P_{o\,ATP}^*$ 0.62 ± 0.03 vs. 0.64 ± 0.03) between spontaneous moderate-P_o channels and channels oxidized to the moderate-P_o state (see Table 1).

Figure 3 illustrates one experiment in which a complete ATP curve was obtained before and after oxidation of the same single channel. The channel presented spontaneously low-P_o behavior, as exemplified by channel activity at 10 μM [Ca^{2+}] (Fig. 3, *first left trace*). After we studied channel response to different concentrations of ATP, the *cis* side of the bilayer was extensively washed. P_o returned to the values shown before ATP exposure. After 90 s of exposure to 20 μM thimerosal, the SH reagent was washed from the *cis* side and the same [ATP] used before oxidation were tested. Figure 3 (*first right trace*) shows channel activity at 10 μM [Ca^{2+}], indicating a change from low-P_o to moderate-P_o calcium dependence (compare with Fig. 3, *first left trace*). Before oxidation, 0.03 mM ATP slightly

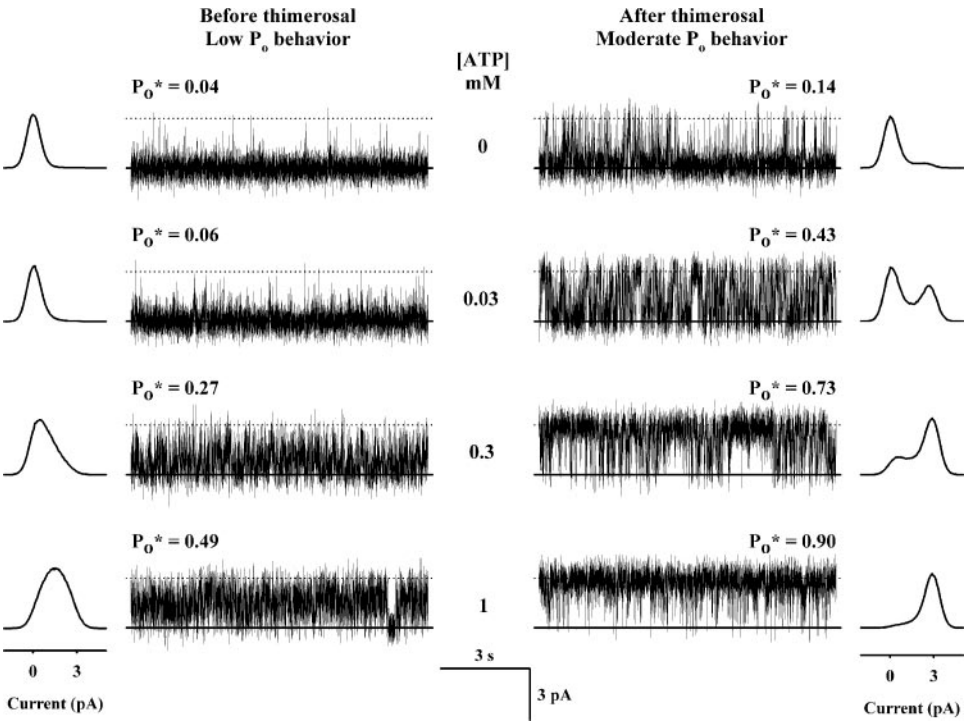

Fig. 3. Differential activation by ATP of a single RyR channel before (*left*) and after (*right*) treatment with thimerosal. Representative current records were obtained at 10 μM cytoplasmic free [Ca^{2+}] at the indicated [ATP]. Average P_o^* values, calculated from at least 150 s of continuous records, are shown. Current histograms of the whole record are shown beside each trace.

increased channel P_o^* from 0.04 to 0.06, whereas after oxidation it markedly increased P_o^* from 0.14 to 0.43 (Fig. 3, *second traces*, *left* and *right*). Similarly, higher changes in P_o were observed after oxidation than before oxidation at 0.3 and 1 mM ATP (Fig. 3, *third* and *fourth traces*, *left* and *right*). Therefore, differential activation by ATP of low-P_o and moderate-P_o channels could be obtained in the same single channel before and after oxidation. Similar results were obtained in three other experiments, two performed with thimerosal and one with DTDP.

Activation by ATP at resting [Ca^{2+}]. To analyze the activation by ATP of RyR channels at [Ca^{2+}] near the resting state of the cell, we performed experiments at 0.1 μM free [Ca^{2+}]. Figure 4 shows the activation by ATP of a low-P_o channel before (Fig. 4*A*) and after (Fig. 4*B*) 120-s exposure to 10 μM thimerosal. After incubation with thimerosal, the channel displayed high-P_o behavior (Fig. 4*B*, *first trace*). P_o values were near 1, both at 10 and 500 μM free [Ca^{2+}] (not shown). The same [ATP] induced much higher activation of the oxidized channel compared with the same channel before oxidation (Fig. 4, *A* and *B*). High-P_o channels showed a decrease in K_{aATP} (from 1,300 μM in low-P_o channels to ~120 μM in high-P_o channels) and a marked increase in maximal P_o change (from 0.1 in low-P_o channels to 0.5 in high-P_o channels; Fig. 4*C*). Note that after oxidation the channel displayed clearly defined open and closed states.

Reversibility of ATP activation. In a recent report Dulhunty et al. (17) showed irreversible activation by ATP of skeletal RyR1 channels suggesting channel phosphorylation. To control for the possibility that phosphorylation of the channels occurred in our experimental setting, we performed the following experiment, with a low-P_o (Fig. 5, *top panels*) and a moderate-P_o channel (Fig. 5, *bottom panels*). After a control period at 10 μM [Ca^{2+}] (Fig. 5, *left panels*), the channels were exposed to 3 mM ATP for 8 min (Fig. 5, *center panels*) and then thoroughly washed and recorded again at 10 μM [Ca^{2+}] (Fig. 5, *right panels*). Channel activity remained stable during the whole period of exposure to ATP. Moreover, after ATP removal, channel activity returned to the level before ATP treatment. Therefore, we consider that, in our experimental conditions, the effect of ATP is not due to phosphorylation.

Noise analysis. It is apparent in Fig. 3 that after oxidation the open and closed states are better defined than before oxidation. This is especially manifest when the current histograms before oxidation and after oxidation are compared at P_o^* near 0.5. Before oxidation the histogram consists of a broad single peak (Fig. 3, *fourth left histogram*), where the frequencies of intermediate current values between the closed and full open states are favored. In contrast, after oxidation two peaks are clearly distinguishable, corresponding to the closed and full open states, with much less frequent intermediate current levels (Fig. 3, *second right histogram*).

To further analyze the change in gating induced by oxidation, we performed noise analysis of the channel current fluctuations. Figure 6 shows the current variance as a function of mean channel current, measured at 1-s intervals, obtained from the channel of the experiment shown in Fig. 3 before and after oxidation at 10 μM [Ca^{2+}]. To obtain the full range of mean current from the closed to the full open state, data obtained at [ATP] ranging from 0 to 3 mM were included. It is apparent that both before and after oxidation the same maximal mean current was attained. Data were fitted

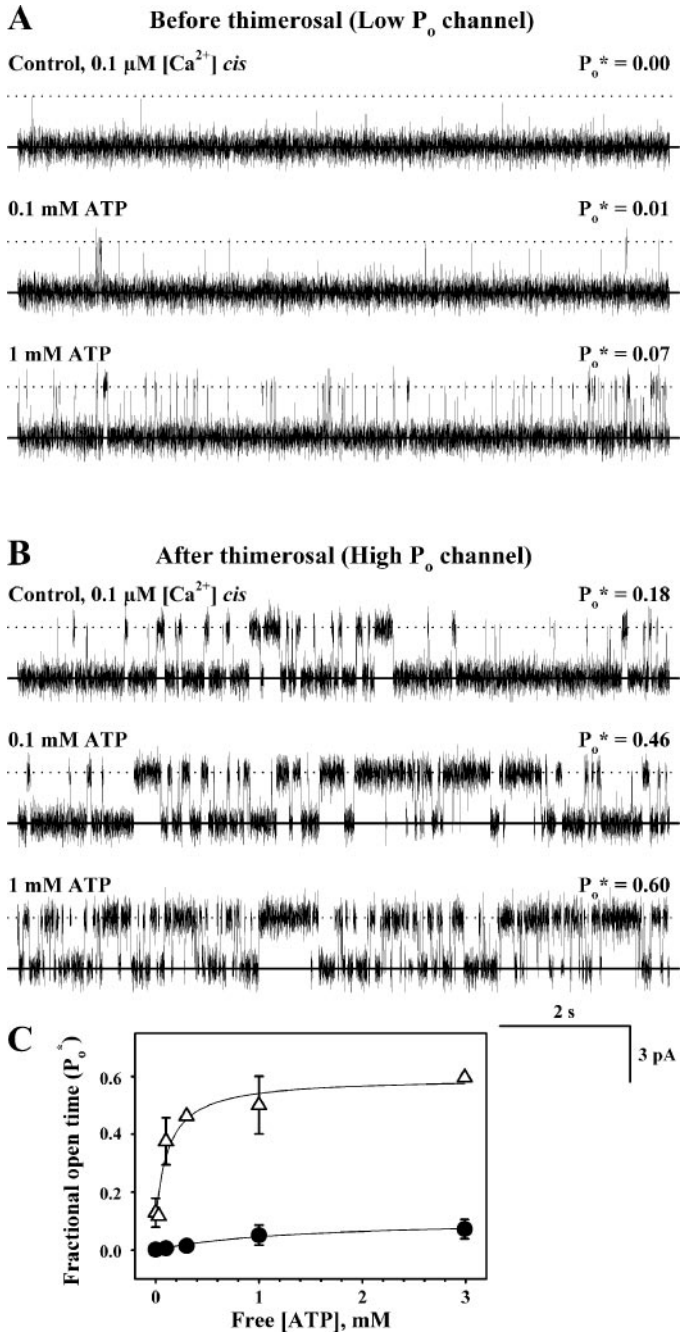

Fig. 4. Differential activation by ATP of single RyR channels at 0.1 μM [Ca^{2+}]. *A* and *B*: representative current records of the same RyR channel were obtained at 0.1 μM cytoplasmic free [Ca^{2+}] at the indicated [ATP] before (*A*) and after (*B*) thimerosal. Average P_o^* values calculated from at least 120 s of continuous records are shown. Note the near absence of substates after oxidation. *C*: mean P_o values of 8 low-P_o channels (●) and of 2 high-P_o channels (△) recorded at the indicated [ATP]. Symbols represent means ± SE for low-P_o channels and means ± value range for high-P_o channels. Solid lines represent the best nonlinear fits to *Eq. 2* (see text).

(solid lines through the symbols) with the following parabolic equation (47)

$$\text{variance} = \text{variance}_b + i * \langle I \rangle - \langle I \rangle^2/n \qquad (3)$$

where $\langle I \rangle$ is the mean current value and variance_b is the current variance independent of channel activity. Assuming identical and independent conducting units, i corresponds to the unitary current and n to the number of conducting units.

The unitary current calculated by noise analysis was 0.75 ± 0.01 pA (estimate ± SE of the estimate) before oxidation and 1.68 ± 0.01 pA after oxidation. These values were about one-fourth and one-half of the full open channel current before and after oxidation, respectively. Because maximal mean current was the same before and after oxidation, the number of conducting levels (n) decreased accordingly from 4.03 ± 0.04 before oxidation to 1.80 ± 0.01 after oxidation. The product $i \times n$, both before and after oxidation, was near 3 pA, similar to I_{max}, the current flowing through full open channel, measured as described in MATERIALS AND METHODS (2.90 ± 0.06 pA, mean ± SD). Noise analysis of the experiment shown in Fig. 4, *A* and *B*, performed at 0.1 μM [Ca^{2+}], yielded a unitary current of 2.59 ± 0.01 pA and n of 1.05 ± 0.00 (estimate ± SE of the estimate) both before and after oxidation.

DISCUSSION

Activation by ATP. ATP applied to the cytoplasmic compartment reversibly activated RyR channels from the ER of rat brain cortex incorporated in planar lipid bilayers. ATP differentially activated RyR channels depending on their calcium response. Channels that showed low-P_o calcium dependence presented lower apparent affinity to activation by ATP than channels that showed moderate-P_o calcium dependence. In a recent report by Oba et al. (43) RyR channels purified from rabbit skeletal muscle were activated by an ATP analog. They found activation of "high-P_o" channels, but not of "low-P_o" channels. The level of activity of their high-P_o and low-P_o channels is similar to that of our moderate-P_o and low-P_o channels, respectively. A possible explanation of the absence of activation of low-P_o channels in their experiments could be that the level of reduction of their low-P_o channels is higher than ours and therefore no activation by ATP could be observed. Sun et al. (52) reported that each RyR subunit has several critical SH residues, the oxidation of which modifies the response to agonists.

In our experiments, channel activity remained stable during the whole recording period at each [ATP]. Spontaneous increases in channel activity, occasionally observed, could arise from oxidation induced by the ambient oxygen tension present during the experiment (19). Therefore, only stable records were included in the analysis. Moreover, the effect of ATP could be reversed by removal of ATP from the chamber; the activity after long exposures to ATP (see Fig. 5) returned to the values observed before ATP exposure. Therefore, we rule out the possibility that the activation by ATP of RyR channels in our experimental conditions is due to phosphorylation as reported by Dulhunty et al. (17) for native RyR channels from skeletal muscle.

Low-P_o channels that attained moderate-P_o behavior after oxidation with thimerosal or DTDP at 10 μM

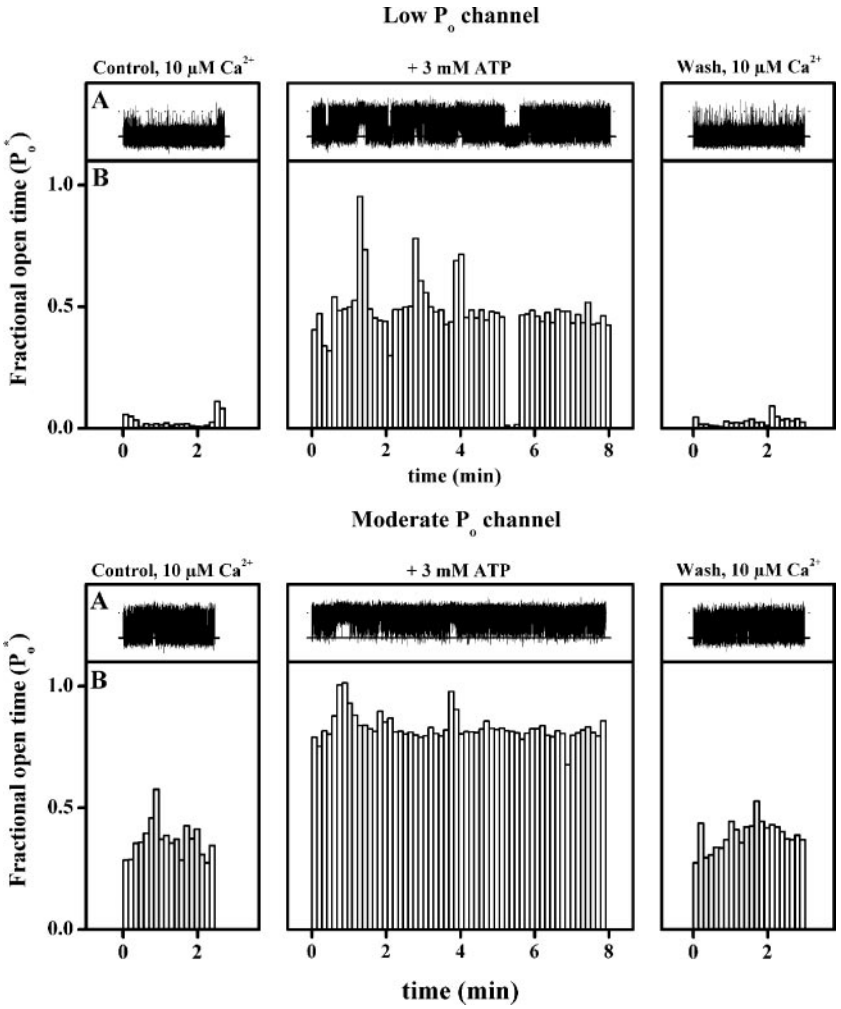

Fig. 5. Reversibility of ATP activation of a low-P_o and of a moderate-P_o RyR channel. *A*: current traces of a low-P_o channel (*top panels*) and a moderate-P_o channel (*bottom panels*) recorded for the indicated time before ATP application (*left panels*), during ~8 min of exposure to 3 mM [ATP] (*center panels*), and after extensive washing of ATP from the *cis* compartment (*right panels*). The channels open upward with a maximal current of 2.9 pA. *B*: P_o^* of the channels recorded in *A* measured in successive intervals of 8.192 s each.

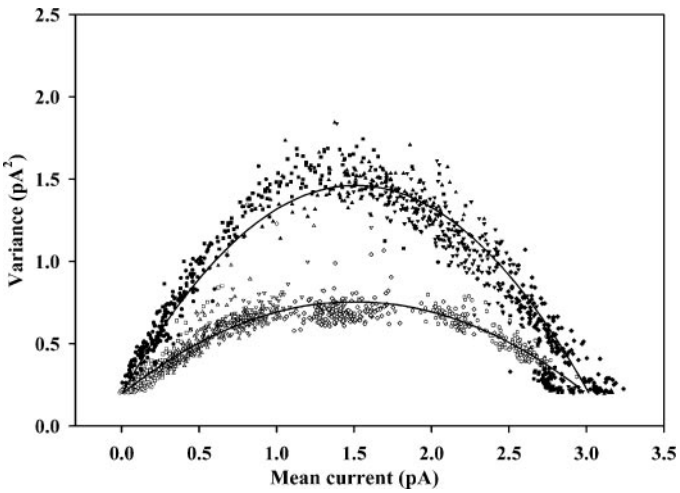

Fig. 6. Noise analysis of the single-channel experiment depicted in Fig. 3. Symbols represent current variance as a function of mean current in successive periods lasting 1 s of channel activity before (open symbols) and after (filled symbols) treatment with thimerosal at different [ATP]: circles, 0 mM; squares, 0.03 mM; triangles, 0.1 mM; inverted triangles, 0.3 mM; diamonds, 1 mM; hexagons, 3 mM. Solid lines through the symbols represent the best least-square fit to *Eq. 3* (see RESULTS).

[Ca^{2+}] increased their apparent affinity for ATP fivefold. The activation by ATP of the oxidized channels was the same, both in extent and in affinity, as that exhibited by channels that spontaneously presented moderate-P_o behavior. Therefore, oxidation of critical hyperreactive SH groups would produce a channel with higher apparent affinity for different agonists such as ATP, calcium, and caffeine (35, 43). This channel behavior may be present in vivo, leading to the possibility that channel oxidation is a physiologically relevant mechanism. It could be argued that at high [ATP] and [Ca^{2+}] both low- and moderate-P_o channels would be maximally activated, making the change in apparent affinity irrelevant. However, fractional open time at those conditions is higher in moderate-P_o channels (0.9) than in low-P_o channels (0.6). Therefore, oxidation would induce a higher degree of calcium release. Moreover, the response of RyR channels to ATP depended on cytoplasmic [Ca^{2+}]; at 0.1 μM [Ca^{2+}] the response to ATP of low-P_o channels was negligible, whereas after oxidation it was pronounced in extent and apparent affinity (see Fig. 4). Therefore, at resting [Ca^{2+}] the effect of oxidation is even more relevant than at 10 μM [Ca^{2+}].

The vesicle preparation used in our experiments contains the three RyR isoforms expressed in rat brain (14, 23), as measured by Western blot with specific antibodies, RyR-2 being by far the most abundant isoform (C. Hidalgo and A. Humeres, personal communication). At equal probability of incorporation (which is not known), RyR-2 is expected to be the isoform most frequently incorporated into the bilayer. However, RyR channels from brain tissue behave differently from those of cardiac tissue, because the most frequent response to calcium in brain is low-P_o behavior, which is never observed in cardiac channels (12, 34, 35). Therefore, the brain channels studied in the present work might be RyR-2 channels with regulatory mechanisms different from those from cardiac muscle, such as FKBP association (11) or redox state. However, we cannot exclude the possibility that they correspond to RyR-1 or RyR-3 channels, and it is possible that the two different channel responses to ATP described in this work could arise from different RyR channel isoforms. However, this interpretation is unlikely, because both types of activation by ATP were obtained in the same single channel at two different oxidation states. Although we do not know which RyR channel isoform was incorporated into the bilayer, we are reasonably confident that the same isoform (the same channel) displayed both responses to ATP, one before and one after oxidation.

The K_{aATP} value we obtained at 10 μM [Ca^{2+}] with low-P_o channels from rat brain cortex (0.42 mM) is similar to the K_{aATP} values published in other tissues. Laver et al. (31) found a single K_{aATP} of 0.36 mM in RyR channels from rabbit skeletal muscle, and Kermode et al. (30) found a K_{aATP} of 0.22 mM in cardiac RyR channels. Jóna et al. (27) found biphasic activation by ATP in channels from rat skeletal muscle, with two K_{aATP} values, one of 0.019 mM and another of 0.35 mM, which are of the same order of magnitude as those obtained with moderate-P_o and low-P_o channels in our experiments, respectively. We did not find cooperativity in channel activation by ATP, neither fitting average data nor fitting data of individual experiments with more than four ATP concentrations (not shown). In RyR channels from cardiac (30) and skeletal (31) muscle, Hill coefficients for ATP activation of 1.5 or 2–4, respectively, have been reported. If we assume that channel subunits gate in an uncoordinated fashion, as seems to be the case in low-P_o channels observed in this work at 10 μM [Ca^{2+}] (see below), no cooperativity should be expected.

Noise analysis. RyR channels from skeletal and cardiac muscle display multiple subconductance states, especially in the absence of FKBP (8, 28, 33, 37, 38, 44, 49). Because of the difficulty in resolving the possible channel substates in our recording conditions, the low signal-to-noise ratio, and the fast kinetics observed in the presence of ATP at 10 μM [Ca^{2+}], we performed noise analysis of channel current fluctuations. The analysis revealed an n of 4 and an i of 0.75 pA for low-P_o channels. One simple interpretation of this result is that, in low-P_o RyR channels, the four subunits function in an uncoordinated fashion, giving rise to evenly spaced current levels. A pattern with four open current levels (¼, ½, ¾, and 1 times the maximal channel current), such as that predicted by our noise analysis, was described in purified skeletal muscle (33, 49) and in RyR channels expressed heterologously without FKBP12 (8, 44). Our noise analysis results could imply that a single RyR channel has four conducting units, each carrying one-fourth of the single-channel maximal current. This can be interpreted as an indication that each of the four subunits can conduct and gate independently, as proposed by Liu et al. (33) and Ondrias et al. (44). Alternatively, the possibility that the four subunits function stochastically to form a single pore, giving rise to evenly spaced current levels, cannot be ruled out.

After oxidation, our noise analysis results indicate that brain RyR channel unitary current is one-half of single-channel maximal current and that the number of conducting units has decreased from 4 to 2. Assuming the existence of subchannels, this result implies that on oxidation the subchannels gate with a certain degree of coordination. One possibility to explain an n of 2 and an i of $½I_{max}$ is that subchannels function in pairs after oxidation. This mode would give rise to three current levels: zero current for the closed state, $½I_{max}$, and I_{max}. This model is consistent with a report showing that the most frequent substate in the purified RyR channel has one-half the maximal conductance of the channel (33). In our experiments, however, current histograms show that the probability of half-maximal current is small (Fig. 3, *right histograms*). Therefore, SH oxidation seems to induce a certain degree of concerted operation of the four channel subunits, favoring the full open and closed states and making substates less probable. The change in gating mode in our experimental conditions is clearly due to oxidation and not to phosphorylation. As can be noted in Fig. 6, even at the highest [ATP] tested, the data obtained before oxidation fall on the parabola representing four conducting units. After oxidation, even before the addition of ATP, the data fall on the parabola of two conducting units. The abundance of substates in our experiments at 10 μM [Ca^{2+}] could be due to the fact that FKBP12 is not tightly associated to RyR channels in brain tissue (11). Whether redox-related changes in subunit coordination involve interactions of FKBP12 with the RyR channel protein remains to be investigated.

Noise analysis of the low-P_o channel at 0.1 μM [Ca^{2+}] revealed the absence of substates. Therefore, no change in coordination could be observed after oxidation. The explanation for this finding is currently under investigation. At 10 μM [Ca^{2+}], oxidation induced both a coordinated function of channel subunits and an increase in apparent affinity for ATP. It is conceivable that to attain the full open state of an uncoordinated channel (the 4 subunits gating independently), binding of ATP to each subunit is required. Instead, in a perfectly coordinated channel, binding of ATP to a single subunit could be sufficient to induce the full open state. However, the results obtained at low [Ca^{2+}] indicate

that at least at 0.1 μM, both effects, subunit coordination and increase in affinity, are not causally related. Thus calcium activation seems to be needed to observe channel substates.

From the results reported in this study, it is proposed that RyR channels from rat brain activated by ATP and calcium function as four independent subchannels in the reduced state. Oxidation induces a coordination in the gating of the subchannels. The redox state of critical SH groups of brain RyR channels controls their response to ATP (43), as it does for cytoplasmic Ca^{2+} (35) and caffeine (43). Changes in intracellular redox potential could modify neuronal processes that depend on calcium release from the ER, including long-term potentiation and long-term depression and presumably learning and memory (3, 5, 6, 24). On the other hand, oxidative stress may enhance CICR in neurons, because oxidation not only increases RyR channel response to calcium and ATP but also suppresses the inhibition of skeletal RyR channels exerted by Mg^{2+} (15). Oxidative stress and alterations in Ca^{2+} homeostasis have been proposed to contribute to neuronal apoptosis and excitotoxicity that could underlie the pathogenesis of several neurodegenerative disorders and stroke (7, 29, 39, 56).

We thank Marco A. Córdova for skillful help with the experiments and Dr. Cecilia Hidalgo for helpful criticism of the manuscript.

This study was supported by Fondo Nacional de Investigación Científica y Tecnológica (FONDECYT) Grant 8980009 and Fondo de Investigación Avanzada en Áreas Prioritarias Grant 15010006.

REFERENCES

1. **Abramson JJ and Salama G.** Sulfydryl oxidation and Ca^{2+} release from sarcoplasmic reticulum. *Mol Cell Biochem* 82: 81–84, 1988.
2. **Abramson JJ, Zable AC, Favero TG, and Salama G.** Thimerosal interacts with the Ca^{2+} release channel ryanodine receptor from skeletal muscle sarcoplasmic reticulum. *J Biol Chem* 270: 29644–29647, 1995.
3. **Alkon DL, Nelson TJ, Zhao W, and Cavallaro S.** Time domains of neuronal Ca^{2+} signaling and associative memory: steps through a calexcitin, ryanodine receptor, K^+ channel cascade. *Trends Neurosci* 21: 529–537, 1998.
4. **Ashley RH.** Activation and conductance properties of ryanodine-sensitive calcium channels from brain microsomal membranes incorporated into planar lipid bilayers. *J Membr Biol* 111: 179–189, 1989.
5. **Berridge MJ.** Neuronal calcium signaling. *Neuron* 21: 13–26, 1998.
6. **Berridge MJ, Lipp P, and Bootman MD.** The versatility and universality of calcium signalling. *Nat Rev Mol Cell Biol* 1: 11–21, 2000.
7. **Bonfoco E, Krainc D, Ankarcrona M, Nicotera P, and Lipton SA.** Apoptosis and necrosis: two distinct events induced, respectively, by mild and intense insults with *N*-methyl-D-aspartate or nitric oxide/superoxide in cortical cell cultures. *Proc Natl Acad Sci USA* 92: 7162–7166, 1995.
8. **Brillantes AB, Ondrias K, Scott A, Kobrinsky E, Ondriasova E, Moscella MC, Jayaraman T, Landers M, Ehrlich BE, and Marks AR.** Stabilization of calcium release channel (ryanodine receptor) function by FK506-binding protein. *Cell* 77: 513–523, 1994.
9. **Bull R and Marengo JJ.** Calcium-dependent halothane activation of sarcoplasmic reticulum calcium channels from frog skeletal muscle. *Am J Physiol Cell Physiol* 266: C391–C396, 1994.
10. **Carafoli E.** Calcium signaling: a tale for all seasons. *Proc Natl Acad Sci USA* 99: 1115–1122, 2002.
11. **Carmody M, Mackrill JJ, Sorrentino V, and O'Neill C.** FKBP12 associates tightly with the skeletal muscle type 1 ryanodine receptor, but not with other intracellular calcium release channels. *FEBS Lett* 505: 97–102, 2001.
12. **Chu A, Fill M, Stefani E, and Entmann ML.** Cytoplasmic Ca^{2+} does not inhibit the cardiac muscle sarcoplasmic reticulum ryanodine receptor Ca^{2+} channel, although Ca^{2+}-induced Ca^{2+} inactivation of Ca^{2+} release is observed in native vesicles. *J Membr Biol* 135: 49–59, 1993.
13. **Copello JA, Barg S, Onoue H, and Fleischer S.** Heterogeneity of Ca^{2+} gating of skeletal muscle and cardiac ryanodine receptors. *Biophys J* 73: 141–156, 1997.
14. **Coronado R, Morrissette J, Sukhareva M, and Vaughan DN.** Structure and function of ryanodine receptors. *Am J Physiol Cell Physiol* 266: C1485–C1504, 1994.
15. **Donoso P, Aracena P, and Hidalgo C.** Sulfydryl oxidation overrides Mg^{2+} inhibition of calcium-induced calcium release in skeletal muscle triads. *Biophys J* 79: 279–286, 2000.
16. **Donoso P, Rodríguez P, and Marambio P.** Rapid kinetic studies of SH oxidation-induced calcium release from sarcoplasmic reticulum vesicles. *Arch Biochem Biophys* 341: 295–299, 1997.
17. **Dulhunty AF, Laver D, Curtis SM, Pace S, Haarmann C, and Gallant E.** Characteristics of irreversible ATP activation suggest that native skeletal ryanodine receptors can be phosphorylated via an endogenous CaMKII. *Biophys J* 81: 3240–3252, 2001.
18. **Eager KR, Roden LD, and Dulhunty AG.** Actions of sulfhydryl reagents on single ryanodine receptor Ca^{2+}-release channels from sheep myocardium. *Am J Physiol Cell Physiol* 272: C1908–C1918, 1997.
19. **Eu JP, Sun J, Xu L, Stamler JS, and Meissner G.** The skeletal muscle calcium release channel: coupled O_2 sensor and NO signaling functions. *Cell* 102: 499–509, 2000.
20. **Favero TG, Zable AC, and Abramson JJ.** Hydrogen peroxide stimulates the Ca^{2+} release channels from skeletal sarcoplasmic reticulum. *J Biol Chem* 270: 2557–2563, 1995.
21. **Feng W, Liu G, Allen PD, and Pessah IN.** Transmembrane redox sensor of ryanodine receptor complex. *J Biol Chem* 275: 35902–35907, 2000.
22. **Fill M, Coronado R, Mickelson JR, Vilveen J, Ma J, Jacobson BA, and Louis CF.** Abnormal ryanodine receptor channels in malignant hyperthermia. *Biophys J* 50: 471–475, 1990.
23. **Furuichi T, Khoda K, Miyawaki A, and Mikoshiba K.** Intracellular channels. *Curr Opin Neurobiol* 4: 294–303, 1994.
24. **Futatsugi A, Kato K, Ogura H, Li ST, Nagata E, Kuwajima G, Tanaka K, Itohara S, and Mikoshiba K.** Facilitation of NMDAR-independent LTP and spatial learning in mutant mice lacking ryanodine receptor type 3. *Neuron* 24: 701–713, 1999.
25. **Giannini G and Sorrentino V.** Molecular structure and tissue distribution of ryanodine receptor calcium channels. *Med Res Rev* 15: 313–323, 1995.
26. **Jayaraman T, Brillantes AM, Timerman AP, Fleischer S, Erdjument-Bromage H, Tempst P, and Marks AR.** FK506 binding protein associated with the calcium release channel (ryanodine receptor). *J Biol Chem* 267: 9474–9477, 1992.
27. **Jóna L, Szegedi C, Sárközi P, and Szentesi P.** Altered inhibition of the rat skeletal ryanodine receptor/calcium release channel by magnesium in the presence of ATP. *Pflügers Arch* 441: 729–738, 2001.
28. **Kaftan E, Marks AR, and Ehrlich BE.** Effects of rapamycin on ryanodine receptor/Ca^{2+}-release channels from cardiac muscle. *Circ Res* 78: 990–997, 1996.
29. **Kelliher M, Fastbom J, Cowburn RF, Bonkale W, Ohm TG, Ravid R, Sorrentino V, and O'Neill C.** Alterations in the ryanodine receptor calcium release channel correlate with Alzheimer's disease neurofibrillary and β-amyloid pathologies. *Neuroscience* 92: 499–513, 1999.

30. **Kermode H, Williams AJ, and Sitsapesan R.** The interactions of ATP, ADP, and inorganic phosphate with the sheep cardiac ryanodine receptor. *Biophys J* 74: 1296–1304, 1998.
31. **Laver DR, Lenz GKE, and Lamb GD.** Regulation of the calcium release channel from rabbit skeletal muscle by the nucleotides ATP, AMP, IMP and adenosine. *J Physiol* 537: 763–778, 2001.
32. **Liu G, Abramson JJ, Zable AC, and Pessah IN.** Direct evidence for the existence and functional role of hyperactive sulfhydryls on the ryanodine receptor-triadin complex selectively labeled by the coumarin maleimide 7-diethylamino-3–4′-(maleimidylphenyl)-4-methylcoumarin. *Mol Pharmacol* 45: 189–200, 1994.
33. **Liu QY, Lai FA, Rousseau E, Jones RV, and Meissner G.** Multiple conductance states of the purified calcium release channel complex from skeletal sarcoplasmic reticulum. *Biophys J* 55: 415–424, 1989.
34. **Marengo JJ, Bull R, and Hidalgo C.** Calcium dependence of ryanodine-sensitive calcium channels from brain cortex endoplasmic reticulum. *FEBS Lett* 383: 59–62, 1996.
35. **Marengo JJ, Hidalgo C, and Bull R.** Sulfhydryl oxidation modifies the calcium dependence of ryanodine-sensitive calcium channels. *Biophys J* 74: 1263–1277, 1998.
36. **Marengo JJ, Viejo L, and Bull R.** Redox-dependent calcium response of brain cortex RyR-channels determines their activation by cADPR and ATP (Abstract). *Biophys J* 76: A376, 1999.
37. **Marx SO, Gaburjakova J, Gaburjakova M, Henrikson C, Ondrias K, and Marks AR.** Coupled gating between cardiac calcium release channels (ryanodine receptors). *Circ Res* 88: 1151–1158, 2001.
38. **Marx SO, Ondrias K, and Marks AR.** Coupled gating between individual skeletal muscle Ca^{2+} release channels (ryanodine receptors). *Science* 281: 818–821, 1998.
39. **Mattson MP, LaFerla FM, Chan SL, Leissring MA, Shepel PN, and Geiger JD.** Calcium signaling in the ER: its role in neuronal plasticity and neurodegenerative disorders. *Trends Neurosci* 23: 222–229, 2000.
40. **McPherson PS and Campbell KP.** Characterization of the major brain form of the ryanodine receptor/Ca^{2+} release channel. *J Biol Chem* 268: 19785–19790, 1993.
41. **Meissner G.** Ryanodine receptor/Ca^{2+} release channels and their regulation by endogenous effectors. *Annu Rev Physiol* 56: 485–508, 1994.
42. **Murayama T and Ogawa Y.** Characterization of type 3 ryanodine (RyR3) of sarcoplasmic reticulum from rabbit skeletal muscles. *J Biol Chem* 272: 24030–24037, 1997.
43. **Oba T, Murayama T, and Ogawa Y.** Redox states of type 1 ryanodine receptor alter Ca^{2+} release channel response to modulators. *Am J Physiol Cell Physiol* 282: C684–C692, 2002.
44. **Ondrias K, Marx SO, Gaburjakova M, and Marks AR.** FKBP12 modulates gating of the ryanodine receptor calcium release channels. *Ann NY Acad Sci* 853: 149–156, 1998.
45. **Rousseau E, Smith JS, and Meissner G.** Ryanodine modifies conductance and gating behavior of single Ca^{2+} release channel. *Am J Physiol Cell Physiol* 253: C364–C368, 1987.
46. **Schiefer A, Meissner G, and Isenberg G.** Ca^{2+} activation and Ca^{2+} inactivation of canine reconstituted cardiac sarcoplasmic reticulum Ca^{2+}-release channels. *J Physiol* 489: 337–348, 1995.
47. **Sigworth FJ.** The variance of sodium current fluctuations at the node of Ranvier. *J Physiol* 307: 97–129, 1980.
48. **Smith JS, Coronado R, and Meissner G.** Single channel measurements of the calcium release channel from skeletal muscle sarcoplasmic reticulum. *J Gen Physiol* 88: 573–588, 1986.
49. **Smith JS, Imagawa T, Ma J, Fill M, Campbell KP, and Coronado R.** Purified ryanodine receptor from rabbit skeletal muscle is the calcium-release channel of sarcoplasmic reticulum. *J Gen Physiol* 92: 1–26, 1988.
50. **Stoyanovsky DA, Salama G, and Kegan VE.** Ascorbate/iron activates Ca^{2+}-release channels of skeletal sarcoplasmic reticulum vesicles reconstituted in lipid bilayers. *Arch Biochem Biophys* 308: 214–221, 1994.
51. **Suko J, Hellmann G, and Drobny H.** Modulation of the calmodulin-induced inhibition of sarcoplasmic reticulum calcium release channel (ryanodine receptor) by sulfhydryl oxidation in single channel current recordings and [(3)H]ryanodine binding. *J Membr Biol* 174: 105–120, 2000.
52. **Sun J, Xu L, Eu JP, Stamler JS, and Meissner G.** Classes of thiols that influence the activity of the skeletal muscle calcium release channel. *J Biol Chem* 276: 15625–15630, 2001.
53. **Timerman AP, Ogunbumni E, Freund E, Wiederrecht G, Marks AR, and Fleischer S.** The calcium release channel of sarcoplasmic reticulum is modulated by FK-506-binding protein. *J Biol Chem* 268: 22982–22999, 1993.
54. **Xia R, Stangler T, and Abramson JJ.** Skeletal muscle ryanodine receptor is a redox sensor with a well-defined redox potential, which is sensitive to channel modulators. *J Biol Chem* 275: 36556–36561, 2000.
55. **Zahradníková A and Palade P.** Procaine effects on single sarcoplasmic reticulum Ca^{2+} release channels. *Biophys J* 64: 991–1003, 1993.
56. **Zipfel GJ, Babcock DJ, Lee JM, and Choi DW.** Neuronal apoptosis after CNS injury: the roles of glutamate and calcium. *J Neurotrauma* 17: 857–869, 2000.
57. **Zucchi R and Ronca-Testoni S.** The sarcoplasmic reticulum Ca^{2+} channel/ryanodine receptor: modulation by endogenous effectors, drugs and disease states. *Pharmacol Rev* 49: 1–51, 1997.